ResearchGate

See discussions, stats, and author profiles for this publication at: https://www.researchgate.net/publication/337811817

Design and Analysis of a Mechanical Hopping Mechanism Suited for Exploring Low-gravity Environments

Article *in* IEEE Aerospace Conference Proceedings · December 2019

CITATIONS
2

READS
90

4 authors, including:

Himangshu Kalita
The University of Arizona
53 PUBLICATIONS **167** CITATIONS
SEE PROFILE

Jekan Thangavelautham
The University of Arizona
205 PUBLICATIONS **834** CITATIONS
SEE PROFILE

Some of the authors of this publication are also working on these related projects:

CubeSat Technology View project

Space Missions View project

All content following this page was uploaded by Jekan Thangavelautham on 07 December 2019.

The user has requested enhancement of the downloaded file.

Design and Analysis of a Mechanical Hopping Mechanism Suited for Exploring Low-gravity Environments

Himangshu Kalita
University of Arizona
1130 N Mountain Ave
Tucson, AZ 85721
hkalita@email.arizona.edu

Troy M. Jameson
University of Arizona
1130 N Mountain Ave
Tucson, AZ 85721
tjameson@email.arizona.edu

George Stancu
University of Arizona
1130 N Mountain Ave
Tucson, AZ 85721
georgestancu@email.arizona.edu

Jekan Thangavelautham
University of Arizona
1130 N Mountain Ave
Tucson, AZ 85721
jekan@email.arizona.edu

***Abstract*—Exploration of extreme environments, including caves, canyons and cliffs on low-gravity surfaces such as the Moon, Mars and asteroid surfaces can provide insight into the geological history of the solar system, origins of life, and prospects for future habitation and resource exploitation. Although current methods of exploration utilizing wheeled ground rovers have excellent performance on relatively flat, benign, even terrains, they are unsuitable for exploring these extreme environments due to their inability to travers rugged environments as their obstacle traversing capabilities are typically limited to wheel diameter, and reduced traction on low-gravity environments. So, developing small, cost-effective robots that can utilize unconventional mode of mobility through ballistic hopping can overcome these limitations. Our past work has proposed using a spherical robot (SphereX) that achieves ballistic hopping mobility through the use of a miniaturized propulsion system and 3-axis reaction wheel system. In this paper, we present the design and control analysis of a mechanical hopping mechanism that can be used for SphereX. The mechanism is comprised of two mechanical systems to produce its ability to maneuver terrain and achieve mobility through ballistic hopping. On the robot's interior, it consists of an electric gearmotor attached to a set of gears, a spring, and a rubber foot. These components make up the hopping mechanism used to hop the robot by applying a force along the longitudinal axis of the spring between the rubber foot and the ground. However, the robot needs to be oriented in a desired orientation in order to achieve ballistic hopping and intercept a desired target. This is achieved through a secondary mechanical system that consists of three linear actuators each connected to levers which are mounted to the exterior of the robot's shell. The lever and the linear actuator system are used to orient the robot in a desired orientation so that when the hopping mechanism is deployed it will be launched in a ballistic trajectory to intercept a desired target. Although the spring based hopping mechanism provides a constant force, but the lever and linear actuator-based system is used to orient the robot at different angles to produce range in mobility. The robot also consists of electronics and sensors equivalent to current smartphones, an array of guidance, navigation and control sensors, lithium-ion battery-based power system and a volume for science payload.**

978-1-7821-2734-7/20/$31.00 ©2020 IEEE

TABLE OF CONTENTS

1. INTRODUCTION

The recent trend towards small and frequent space missions to the Moon, Mars, other planetary moons, asteroids, and comets has sparked new interest on the development of mobility platforms with dedicated scientific instruments. However, the best method to achieve mobility on planetary bodies is still the subject of discussion. So far, mobile wheeled robots have become integral for surface exploration of the Moon, Mars and other planetary bodies. These rovers have proven their merit, but they are large, in the order of several hundred kilograms and house state-of-the-art science laboratories. Moreover, they can drive over obstacles that are a fraction of the vehicle's body length and uses a significant number of actuators and complex suspension linkages. As such exploration of extreme and rugged environments remains out of reach for current planetary rovers.

The last decade has seen a revolution in the miniaturization of satellites for Low Earth Orbit (LEO) applications. The advent of small satellites and micro-satellites has changed the cost models associated with space operations and has also led to rapid advancement in lightweight structural materials, miniaturization of electronics, sensors and actuators. With these recent developments, it is now possible to develop

small, lightweight and low-cost platforms to tackle some of the hardest challenges in planetary exploration. In our past works we had presented an architecture for a spherical robot called SphereX with several kilograms in mass and several liters in volume that can perform exploration in low-gravity environments through hopping and rolling [1-4]. We proposed the use of a miniaturized propulsion system and a 3-axis reaction wheel system to obtain hopping and rolling mobility. In this paper, we extended our work and present a mechanical hopping mechanism that fits inside the SphereX robot and suited for hopping in lo-gravity environments.

2. Background And Motivation

Small spherical robots have been widely proposed in the past. Their spherical shape enables them to roll on loose, even terrain. Examples include spherical robots developed at Univ. of Sherbrooke [5], Kickbot [6] developed at MIT, Cyclops [7] at Carnegie Mellon University and inflatable ball robots developed at North Carolina State University [8] and University of Toronto [9]. Typically, these spherical robots use a pair of direct drive motors in a holonomic configuration. Others such as the Cyclops and the inflatables pivot a heavy mass, thus moving center of gravity that results in rolling. Other mobility techniques including use of spinning flywheels attached to a two-link manipulator on the Gyrover [10] or 3-axis reaction wheels to spin and summersault as with the Hedgehog developed by Stanford and NASA JPL [11]. Hedgehog's use of reaction wheels enables it to overcome rugged terrain by simply creeping over the obstacle no matter how steep or uneven. However, it's unclear if a gyro-based system can overcome both steep and large obstacles. In reality, even a gyro-based system is bound to slip on steep surfaces, but under low gravity environments such as asteroids, they may be able to reach meters in height.

An alternative to rolling and creeping is hopping. A typical approach to hopping is to use a hopping spring mechanism to overcome large obstacles [12]. One is the Micro-hopper for Mars exploration developed by the Canadian Space Agency [13]. The Micro-hopper has a regular tetrahedron geometry that enables it to land in any orientation at the end of a jump. The hopping mechanism is based on a novel cylindrical scissor mechanism enabled by a Shape Memory Alloy (SMA) actuator. However, the design allows only one jump per day on Mars. Another technique for hopping developed by Plante and Dubowsky at MIT utilize Polymer Actuator Membranes (PAM) to load a spring. The system is only 18 grams and can enable hopping of Microbots with a mass of 100 g up to 1 m [14],[15]. Microbots are cm-scale spherical robots equipped with power and communication systems, a mobility system that enables it to hop, roll and bounce and an array of miniaturized sensors such as imagers, spectrometers, and chemical analysis sensors developed at MIT. They are intended to explore caves, lava tubes, canyons and cliffs. Ideally, many hundreds of these robots would be deployed enabling large-scale in-situ exploration.

SphereX is the direct descendant of the Microbot platform. SphereX has the same goals as the Microbots, but with the goal of launching fewer robots, that are better equipped with science grade instruments.

3. System Design

SphereX is a small, low-cost, modular spherical robot that is designed for exploring extreme environments on low-gravity environments like the Moon, Mars, icy moons and asteroids as shown in Figure 1. It consists of a mobility system to perform optimal exploration of these target environments. It also consists of space-grade electronics like computer board for command and data handling, power board for power management and radio transceiver for communicating among multiple robots. Moreover, it also consists of a power system for power generation/storage, multiple UHF/S-band antennas and accommodates payloads in the rest of the volume. A large rover or lander may carry several of these SphereX robots that can be tactically deployed to explore and access rugged environments inaccessible by it.

Our past work has proposed the use of a miniaturized propulsion system and a 3-axis reaction wheel system to achieve controlled ballistic hopping for mobility. Although propulsive ballistic hopping is the most optimal mode of mobility for long-range exploration in low-gravity environments, we are also interested in mechanical hopping mechanisms for short-range explorations [16]. In this paper, we present the design and control analysis of a mechanical hopping mechanism that can be used for SphereX along with details of other subsystems.

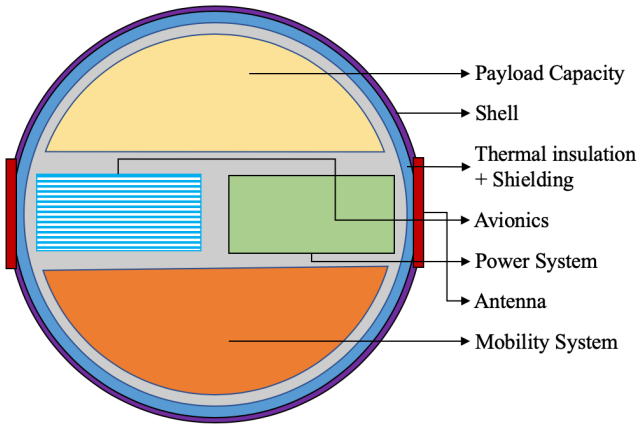

Figure 1. SphereX system architecture

Hopping Mechanism

The mechanical hopping mechanism consists of an electric gear motor attached to a pinion and rack gear system, a spring and a foot as shown in Figure 2 (Left and Middle). The design of the pinion gear is shown in Figure 2(Right), where the teeth subtended by the angle Φ are removed. As such, the mechanism has two phases: a) Compression phase, and b) Release phase. When the pinion gear rotates in a clockwise direction, for a rotation of $2\pi - \Phi$, the rack travels in the upward direction compressing the spring which correspond to the compression phase. Next, as soon as the pinion gear rotates an angle of $2\pi - \Phi$, it unlocks from the rack and the

spring is released to its original length which corresponds to the release phase. Considering D_p as the pitch diameter of the pinion, the displacement of the rack during the compression phase is $\Delta x_r = \pi D_p(2\pi - \Phi)/2\pi$. As such, the spring is compressed by a distance $\Delta x = \Delta x_r$ and the restoring force generated by the spring is equal to $F = k\Delta x$, where k is the spring constant. During the release phase, when the spring is released, the foot hits the ground resulting in the action of a normal force acting on the robot.

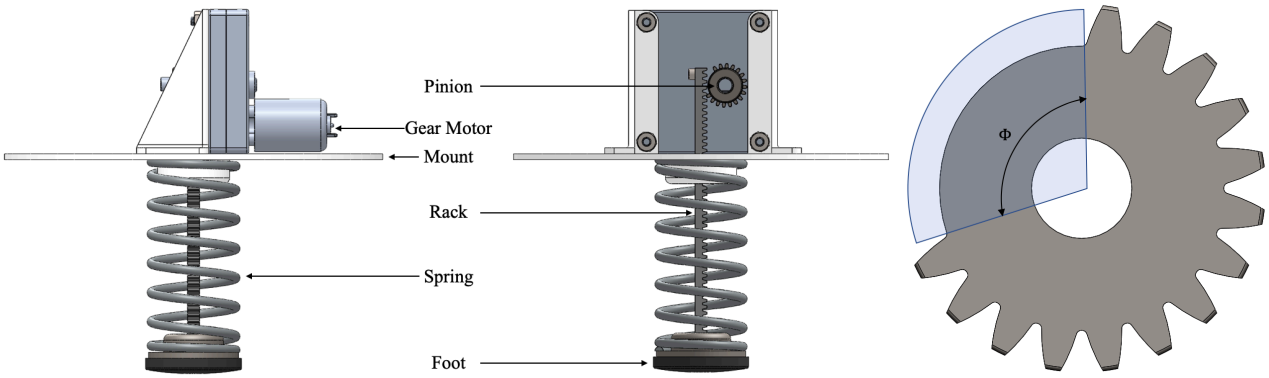

Figure 2. (Left and Middle) Two different views of the hopping mechanism consisting a gear motor, rack and pinion gear system, a spring and a foot, (Right) Design of the pinion gear with the teeth subtended by the angle Φ removed.

Steering Mechanism

Although the mechanism discussed above results in the action of a normal force on the robot, a steering mechanism is still needed to orient the robot at a desired angle so that it can perform ballistic hops. The steering mechanism consists of three linear actuators, each connected to levers which are mounted to the exterior of the robot's chassis (shell) as shown in Figure 3.

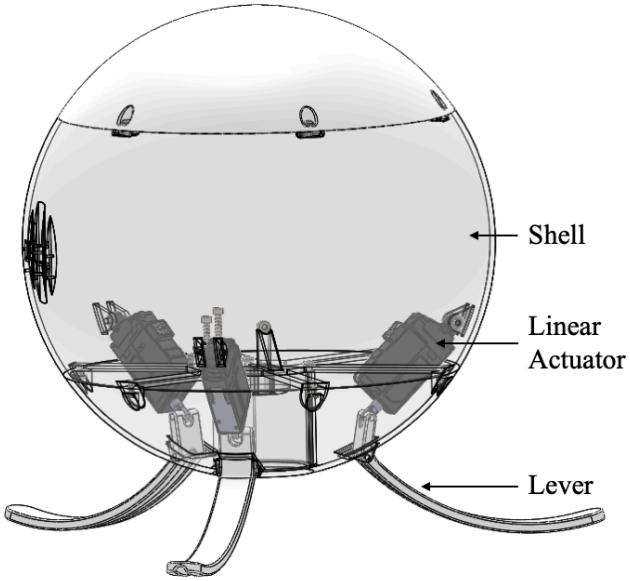

Figure 3. Steering mechanism consisting of three linear actuators, each connected to levers mounted on the robot shell.

By actuating each lever independently, it is possible to position the robot onto the ground and then orient the robot at a desired angle before releasing the spring of the hopping mechanism causing the robot to perform ballistic hops.

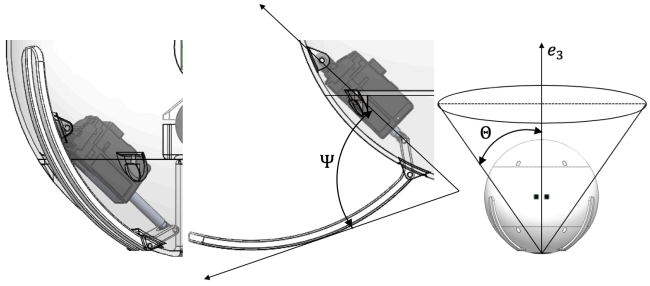

Figure 4. (Left) Position of the lever when the linear actuator is actuated to its full stroke length, (Middle) Position of the lever when the linear actuator is retracted, (Right) Possible orientations of the robot with respect to the vertical axis e_3 defined by the cone with angle Θ.

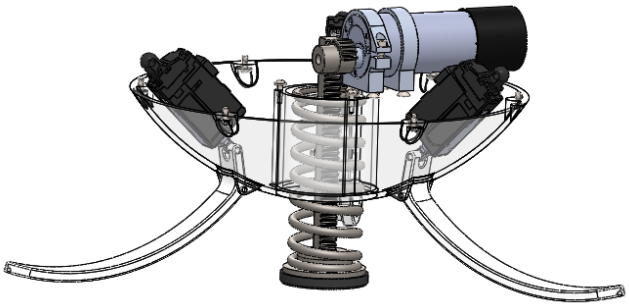

Figure 5. The hopping mechanism and the steering mechanism assembled together inside the lower half of SphereX.

The lever is designed such that it's radius of curvature is equal to the radius of the robot. The orientation of the lever with respect to the axis of actuation of the linear actuator is defined by an angle Ψ, and is a function of the stroke of the linear actuator as shown in Figure 4. As such when the linear actuator is actuated to its full stroke length, $\Psi = 0$, and when the linear actuator is retracted, $\Psi = \Psi_{max}$. Hence, by actuating each linear actuator independently, the robot can be

oriented by an angle $\Theta = f(\Psi_1, \Psi_2, \Psi_3)$, with respect to the vertical axis e_3 defined by a conical section as shown in Figure 4(Right). Figure 5 shows both the hopping and steering mechanism assembled together inside the lower half of SphereX.

Command & Data Handling

The main computer selected for the robot is Rincon Research's AstroSDR which is a complete RF payload: software-defined radio (SDR), FPGA signal processor, ARM processor, and data storage. The single board computer contains the Dual-core ARM Cortex A9 with NEON processor that can operate at up to 733 MHz and a Xilinx Zynq 7045 FPGA. It also contains 512 Mbyte DDR3 RAM memory and 2 GByte Flash for radiation-tolerant OS storage and an option for 64 GByte eMMC flash storage. The tuning range for the receiver and transmitter is 70 MHz to 6 GHz with a maximum bandwidth of 56 MHz. It also has 30 pins 1.8 V GPIO and 24 pins 3.3 V GPIO interfaces. The dimension of the board is 90 x 90 mm, weighs only 95 g, consumes 5.5 W power under nominal conditions and has an operating temperature range of -40°C to 85°C.

Power

Power required for the operation of the robot will be done through NanoPower BP4 battery pack. The battery pack consists of four 18650 series lithium-ion cells resulting in a capacity of 38.5 Wh. The weight of the battery pack is 258 g with dimensions 94 x 84 x 23 mm. Power management will be done through the GomSpace NanoPower P31u board that is configurable with the battery pack. It features a microcontroller that provides maximum power-point tracking (MPPT) capability, measures and logs voltages, currents and temperatures of the system. With an I2C interface, it is possible to read out measurements, control the on/off-state of 3.3 V and 5 V busses, switch on/off the MPPT and to set/read various parameters. The incoming power from the batteries is used to feed two buck-converters supplying a 3.3 V @ 5 A and a 5 V @ 4 A output bus. It also contains six individually controllable output switches with over-current shut-down and latch-up protection, each separately configurable to either 3.3 V or 5.0 V output. The dimension of the board is 89.3 x 92.9 x 15.3 mm, weighs only 100 g and consumes 0.165 W power under nominal conditions.

Communication

With multiple robots deployed to perform cooperative exploration, efficient inter-robot communication is a key factor. The robots need to transmit information with synchronization among them and a communication synchronization protocol will be used, where each robot transmit one at a time and wait for its time to transmit again [4]. To accommodate this protocol, multiple UHF/S band antennas will be used as an array along the circumference of the robot such that the directivity of the array is maximized [4].

Payload

The robot will have a payload capacity of mass 500 g, volume 0.5 liter and power less than 5 W. The payload will be accommodated on the top half of the robot and can include stereo cameras, LiDARs or bio-detection instruments.

4. Modeling Of The Hopping Process

A simplified model is developed for the hopping process as shown in Figure 6. The first step is to compress the spring to store energy $E_0 = k\Delta x^2/2$ (where, k is the spring constant and Δx is the displacement of the spring), the next step is to orient the robot at a desired angle and the last step is to release the stored energy causing the robot to hop. During the last step, the body of the robot first accelerates upward due to the spring force, while the lower part remains stationary. Once the body moves to a specific height, a perfect inelastic collision happens between the body and the foot if the spring constant is large. After the collision, both parts move with the same velocity, which is the robot's take-off velocity v_0.

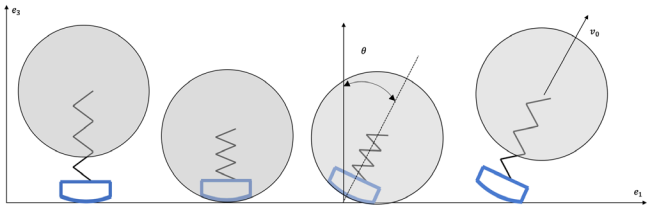

Figure 6. Simplified model of exchange of energy for the hopping process.

Let the mass of the body be m_b and that of the foot be m_f. In the ideal case, all the energy E_0 stored in the spring is converted to the kinetic energy of the body. Therefore, the speed of the body before the inelastic collision is $v_b = \sqrt{2E_0/m_b}$. By the conservation of momentum, $m_b v_b = (m_b + m_f)v_0$, thus the take-off velocity is calculated according to Equation (1).

$$v_0 = \frac{m_b}{m_b + m_f} v_b = \frac{\sqrt{2m_b E_0}}{m_b + m_f} \qquad (1)$$

The kinetic energy at take-off is expressed as Equation (2).

$$E = \frac{1}{2}(m_b + m_f)v_0^2 = \frac{m_b}{m_b + m_f} E_0 = \frac{1}{r+1} E_0 \qquad (2)$$

where, $r = m_f/m_b$ is the mass ratio between the foot and the body. The robot after leaving the ground with the take of velocity v_0 will be subjected to gravitational force and air resistance. If the air resistance is negligible, then the robot performs a projectile motion. With a coordinate frame whose origin is at the take-off point, x-axis along the horizontal direction and z-axis along the vertical direction, the robot's trajectory is given by the Equation (3).

$$x(t) = v_0 t \cos\theta\,, \quad z(t) = v_0 t \sin\theta - \frac{1}{2} g t^2 \qquad (3)$$

where, θ is the take-off angle, and g is the gravitational constant. Based on the trajectory, the hopping height h and distance d can be obtained as Equation (4) and (5).

$$h = \frac{v_0^2}{2g}\sin^2\theta = \frac{E_0 \sin^2\theta}{(1+r)mg} \tag{4}$$

$$d = \frac{v_0^2}{g}\sin 2\theta = \frac{2E_0 \sin 2\theta}{(1+r)mg} \tag{5}$$

where, $m = m_b + m_f$ is the total mass of the robot. From these equations, it can be seen that in order to maximize the hopping height and distance, the mass ratio r and the total mass m should be minimized, while the stored energy E_0 should be maximized. Considering $r \to 0$, since the mass of the body is significantly more than the mass of the foot, our goal is to minimize the total mass m so that the hoping distance d is maximized.

5. Design Analysis

As discussed above, the mass of the robot has to be minimized in order to maximize its hopping distance. Considering the mass of all the other subsystems except the hopping mechanism to be fixed, we analyzed each component of the hopping mechanism to find the optimal design.

Spring Design

For the design of the spring for SphereX, Hooke's law is assumed to hold $F = k\Delta x$, where F is the restoring force exerted by the spring and Δx is the displacement of the spring. The spring constant k can be expressed as a function of the material properties of the spring as Equation (6).

$$k = \frac{G d_w^4}{8 n_a D_c^3} \tag{6}$$

where, G is the material shear modulus, n_a is the number of active coils, D_c is the mean coil diameter and d_w is the wire diameter of the spring. The number of active coils is calculated as $n_a = n_t - n^*$, where n_t is the total number of coils and n^* is the number of end coils. The maximum shear stress $\tau_{max,s}$ occurs on the inner face of the spring coil and is expressed as Equation (7).

$$\tau_{max,s} = \frac{8FWD_c}{\pi d_w^3} \tag{7}$$

where, W is the Wahl correction factor which accounts for shear stress resulting from spring curvature and is expressed as Equation (8).

$$W = \frac{4C-1}{4C-4} + \frac{0.615}{C} \tag{8}$$

where, $C = D_c/d_w$ is the spring index. Considering L_s to be the uncompressed length of the spring, the maximum displacement possible is $\Delta x_{max} = L_s - n_t d_w$. Finally, the mass of the spring can be calculated as $m_s = \pi^2 D_c n_t d_w^2 \rho/4$, where ρ is the density of the material used. Figure 7 shows the spring constant k, mass m_s and maximum shear stress $\tau_{max,s}$ for the spring as a function wire diameter and mean coil diameter for a load of $F = 500$N, $n_t = 10$, and $n^* = 2$. The material used for the design of the spring is Music Wire – ASTM A228 – Spring Wire with a density of $\rho = 7861$ kg/m^3.

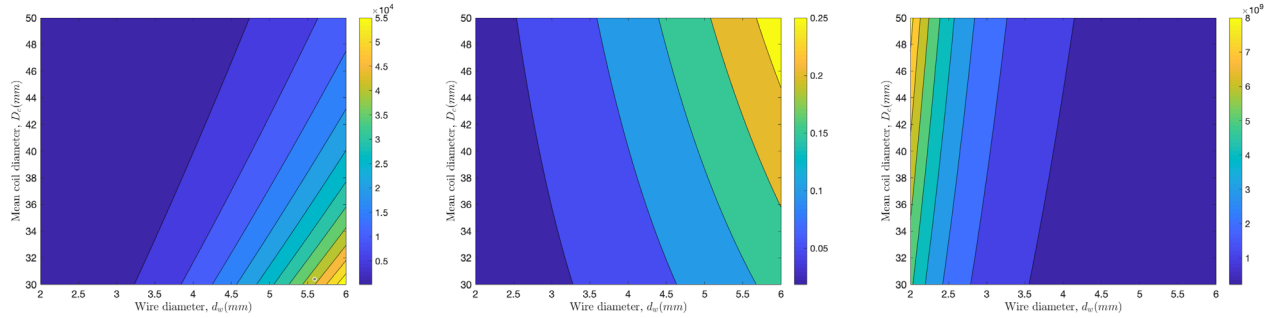

Figure 7. (Left) Spring constant k in N/m, (Middle) Mass of the spring m_s in kg, and (Right) Maximum shear stress on the spring $\tau_{max,s}$ in N/m^2 as a function of wire diameter d_w and mean coil diameter D_c.

Gear Design

The gear system consists of a rack and a pinion. During the compression of the spring, both the rack and the pinion experiences a load equal to $F = k\Delta x$. The classical method of estimating the bending stresses in a gear tooth is the Lewis equation. It models a gear tooth taking the full load at its tip as a simple cantilever beam. The maximum bending stress $\sigma_{max,g}$ developed is given by Equation (9).

$$\sigma_{max,g} = \frac{F_t P}{wY} \tag{9}$$

where, F_t is the tangential tooth load, P is the diametral pitch, w is the face width of tooth, and Y is the Lewis form factor. The Lewis form factor Y is a function of the number of teeth, pressure angle, and involute depth of the gear. The diametral pitch is calculated as $P = N/D_p$, where, N is the number of teeth and D_p is the pitch diameter of the pinion. The rack is designed to have the same face width and pitch as the pinion.

The minimum length of the rack L_r required is equal to sum of the length of the spring and the diameter of the pinion, $L_r = L_s + D_p$. Considering the rack to have a height of pitch H, the mass of the rack and the pinion is then approximated as $m_r = HwL_r\rho$ and $m_p = \pi D_p^2 w\rho/4$, where ρ is the density of the material used.

Moreover, as discussed in Section 3, if the angle subtended by the removed teeth of the pinion is Φ, the maximum displacement of the rack is $\Delta x_r = \pi D_p(2\pi - \Phi)/2\pi$. The design of the angle Φ has to be such that the maximum displacement of the rack is less than or equal to the maximum displacement of the spring $\Delta x_r \leq \Delta x_{max}$. Figure 8 shows the maximum bending stress $\sigma_{max,g}$, mass of the rack m_r and mass of the pinion m_p as a function of pitch diameter D_p and face width w for a load of $F = 500\text{N}$, and $N = 20$. The material used for the design of the rack and pinion is 1045 Carbon Steel with a density of $\rho = 7870\ \text{kg/m}^3$.

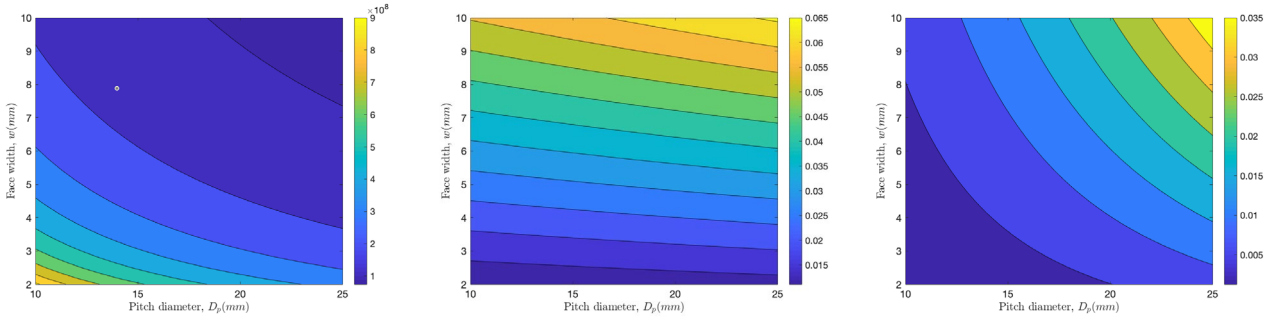

Figure 8. (Left) Maximum bending stress $\sigma_{max,g}$ in N/m^2 on the gear tooth, (Middle) Mass of the rack m_r in kg, and (Right) Mass of the pinion m_p in kg as a function of the pitch diameter D_p and face width w.

Foot Design

When the spring is released and the foot impacts the ground, it will experience a normal force equal to $F = k\Delta x$. The foot is designed as a circular disk of radius r_f and thickness t_f. Assuming the load acting on it during its impact with the ground as a concentrated load at its center, the maximum stress occurs at the center on the lower surface and can be expressed as Equation (10)

$$\sigma_{max,f} = \frac{F}{t_f^2}(1+\nu)\left(0.485\ln\frac{r_f}{t_f} + 0.52\right) \qquad (10)$$

where, ν is the Poisson's ratio of the material used. Thus, the mass of the foot can be approximated as $m_f = \pi r_f^2 t_f \rho$, where ρ is the density of the material used. Figure 9 shows the maximum stress $\sigma_{max,f}$, and mass of the foot m_f as a function of foot radius r_f and foot thickness t_f for a load of $F = 500\text{N}$. The material used for the design of the foot is 2024-T4 Aluminum with a Poisson's ratio $\nu = 0.32$ and density of $\rho = 2780\ \text{kg/m}^3$.

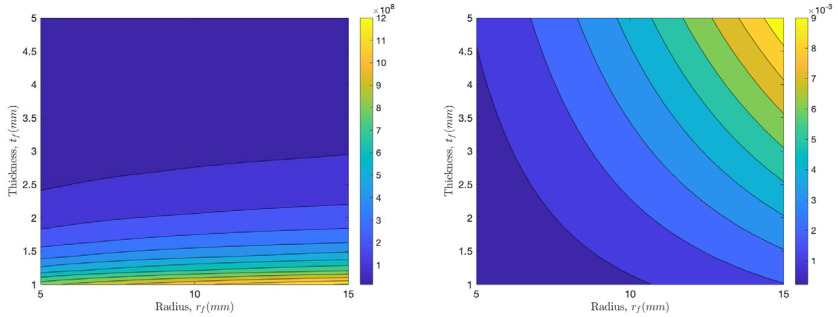

Figure 9. (Left) Maximum stress $\sigma_{max,f}$ in N/m^2, and (Right) Mass of the foot m_f in kg as a function of foot radius r_f and foot thickness t_f.

Motor Selection

With the gear system experiencing a maximum force of F, when the spring is fully compressed, the torque required to rotate the pinion gear is $\mathfrak{m} = FD_p/2$. Thus, a motor is carefully selected such that it can provide a maximum torque greater than $\mathfrak{m}$ and sustain a maximum load greater than F.

Design Optimization

The goal of the optimization process is to minimize the mass of hopping mechanism (spring, gear system and foot) for a given mass of the other subsystems (avionics, power, communication, shell) such that the robot can hop a maximum distance d_{max}, which is user defined. The design variables for the optimization process are $\mathbb{x} =$

$[D_c, d_w, L_s, w, D_p, \Phi, r_f, t_f]$. We have considered the total number of coils of the spring and the number of teeth of the gear as constant. Also, considering the mass of all the other subsystems except the hopping mechanism to be m_o, the total mass of the robot is $m = m_o + m_s + m_r + m_p + m_f$ and mass of the body $m_b = m - m_f$. Five constraints are added to the optimization problem. The first three constraints are such that the stresses developed in the spring, gear and foot are less than 50% of the yield strength of the materials used. The fourth constraint is such that the displacement of the rack is less than or equal to the maximum possible displacement of the spring. And finally, the fifth constraint is such that the hopping distance d of the robot at $\theta = 45°$ is greater than or equal to the user defined maximum distance d_{max}. The problem can be mathematically formulated as Equation (11).

$$\min f(\mathbb{x}) = m_s + m_r + m_p + m_f$$
$$subject\ to \begin{cases} g_1(\mathbb{x}) \equiv \tau_{max,s} \leq 0.5\sigma_{t,s} \\ g_2(\mathbb{x}) \equiv \sigma_{max,g} \leq 0.5\sigma_{t,g} \\ g_3(\mathbb{x}) \equiv \sigma_{max,f} \leq 0.5\sigma_{t,f} \\ g_4(\mathbb{x}) \equiv \Delta x_r \leq \Delta x_{max} \\ g_5(\mathbb{x}) \equiv d \geq d_{max} \end{cases} \quad (11)$$

5. Results And Discussions

With the mathematical model of each element of the hopping mechanism developed and the optimization model defined, we investigated the design of the hopping mechanism for exploration in different environments. Exploration of an environment with SphereX through hopping will be done by employing a Hop+Map→Stop→Science→Process cycle, with each cycle taking 5 minutes. During the Hop+Map phase, the robot hops from its current position to a desired position while performing mapping of the environment. After the hop is completed, the robot stops and performs science operations, processes the collected data and then hops to the next location. Table 1 shows the mass and power consumption of each component of SphereX except the hopping mechanism. The power consumption for the computer & transceiver, power management board, antennas and payload are assumed to be constant throughout the mission. The steering mechanism consumes power only to orient the hop to execute a hop and is calculated to consume an average of 2W per hop. The power consumed by the motor to operate the hopping mechanism will depend on the design solution of the hopping mechanism found through the optimization process and will be discussed later.

Table 1. Mass and power consumption of each component of SphereX except the hopping mechanism

Component	Mass (g)	Power Consumption (W)
Computer + Transceiver	95	5.5
Battery + Power Board	359	0.165
Antennas	120	2
Shell	300	0
Payload	500	5
Steering Mechanism	250	2 (avg)
Motor	300	~
Connectors + Mounting plate	300	0

Table 2 shows the material properties (density and yield strength) used for the design of the spring, gear system and foot of the hopping mechanism.

Table 2. Material properties used for the design of the spring, gear system and foot of the hopping mechanism

Component	Material	Density (kg/m^3)	Yield Strength (MPa)
Spring	Music Wire – ASTM A228	7861	200
Gear	1045 Carbon Steel	7870	310
Foot	2024-T4 Aluminum	2780	324

Exploration on the surface of the Moon

The first target environment for which we analyzed the design of the hopping mechanism is on the surface of the Moon with gravity $g = 1.62\ \mathrm{m/s^2}$. The design optimization is performed such that the robot can hop at least a maximum distance of $d_{max} = 5m$ at an angle of $\theta = 45°$. Form Table 1, the mass of all the other subsystems except the hopping mechanism is $m_o = 2.2$ kg. The bounds for each design variable are $D_c^{(b)} = [10 \quad 50]$ mm, $d_w^{(b)} = [2 \quad 6]$ mm, $L_s^{(b)} = [10 \quad 80]$ mm, $w^{(b)} = [5 \quad 15]$ mm, $D_p^{(b)} = [10 \quad 30]$ mm, $\Phi^{(b)} = [10 \quad 80]$ °, $r_f^{(b)} = [10 \quad 50]$ mm, and $t_f^{(b)} = [1 \quad 10]$ mm. The problem is modeled as a nonlinear optimization problem (NLP) and we used the sequential quadratic programming (SQP) method to solve it. At each iteration of SQP, the gradient is calculated using the finite difference method and the hessian is calculated using the Broyden-Fletcher-Goldfarb-Shanno (BFGS) method. Figure 10 shows the variation of the objective function value, constraint violation and the first-order optimality of the optimization process. It can be seen that the objective function value is stationary, and the constraint violation and the first-order optimality approached zero.

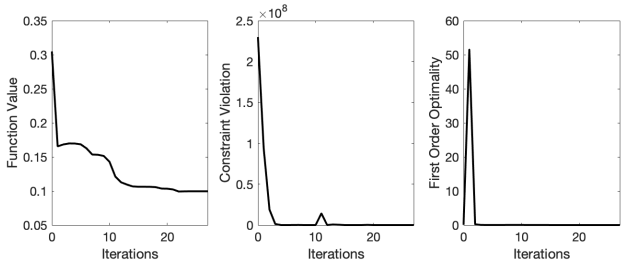

Figure 10. Variation of objective function value, constraint violation and first-order optimality over iterations for the optimization process

Table 3 shows the optimum values of the design variables $\mathbb{x} = [D_c, d_w, L_s, w, D_p, \Phi, r_f, t_f]$ found, and Table 4 shows the mass of the spring, rack, pinion, and foot for the robot to hop a distance of 5m at an angle of 45° on the surface of the Moon.

Table 3. Optimum design variables found through the optimization process

Design Variable	Optimum Value
D_c	22.32 mm
d_w	3.45 mm
L_s	69.7 mm
w	9.48mm
D_p	13.65 mm
Φ	70°
r_f	10.6 mm
t_f	2.35 mm

Table 4. Mass of the components of the hopping mechanism

Component	Mass (g)
Spring	60
Rack	70
Pinion	30
Foot	10

The spring constant for this optimal design is found to be $k = 15.8\ \mathrm{kN/m}$ and the displacement of the spring is $\Delta x = 34.6\ \mathrm{mm}$. As such the maximum restoring force generated by the spring is $F = 546.68\ \mathrm{N}$, and the energy stored in the spring is $E_0 = 9.43\ \mathrm{J}$. Thus, the maximum torque required to rotate the pinion gear is $\mathfrak{m} = 3.73\ \mathrm{Nm}$. Thus, the maximum electrical power consumed by the motor for each hop is given by Equation (12).

$$P_h = \left(i_0 + \frac{\mathfrak{m}}{k_T}\right) V \qquad (12)$$

Where, i_0 is the no load current, k_T is the torque constant, and V is the operating voltage. Using the values of the selected motor and averaging out the power consumption of the motor during the hoping phase into the exploration cycle time of 5 minutes, we found $P_h = 2.3\ \mathrm{W/cycle}$. Thus, with the selected battery pack, the robot will be able to operate for 2.4 hours performing 30 hops and exploring 150 meters on the surface of the Moon. Using this optimal design of the hopping mechanism designed for the Moon, we investigated how the hopping distance varies with gravity. Figure 11 shows the variation of the hopping distance of the optimal design found for the Moon as a function of gravity with the red squares showing the hopping distance on the surface of Callisto, Europa, Ganymede, Moon, Io, and Mars. Although, we showed an optimal design for operation on the surface of the Moon, this method of design optimization can be used to find the optimal design for any planetary surface based on the maximum hopping distance a designer wants.

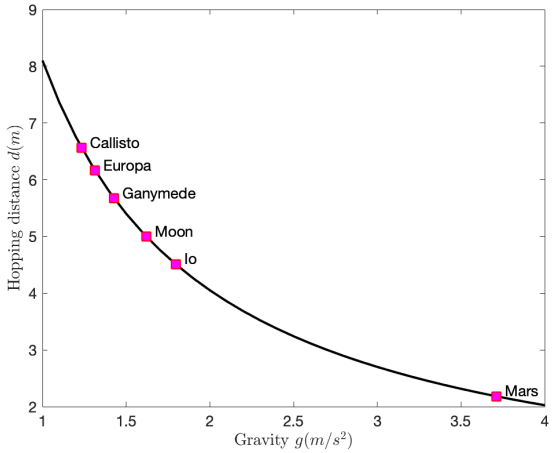

Figure 11. Variation of hopping distance as a function of gravity for the hopping mechanism designed for Moon

6. CONCLUSION

This paper presented an extension of our earlier work on SphereX. SphereX is a hopping robot for exploring low-gravity environments. Our past work dealt with development of a propulsive hopping system with one miniaturized propulsion system and a 3-axis reaction wheel system. In this paper, we presented a design of a mechanical hopping system that consists of a hopping mechanism and a steering mechanism. The hopping mechanism consists of a gearmotor, a rack and pinion gear system, a spring and a foot. Using this system, it is possible to generate normal force on the robot from the ground. The steering system consists of three linear actuators each attached to levers. Operating each linear actuator independently, it is possible to position the robot and orient it at a desired angle. With the steering mechanism and the hopping mechanism operating in coordination, the robot can perform ballistic hops at any desired angle. To analyze the performance of this system, we modeled the hopping process and then developed mathematical design models for the spring, gear system and

the foot. We then developed an optimization model to find the optimal design variables of the spring, gear system and the foot and employed it to design the robot to hop 5 meters on the surface of the Moon. The design found can operate for 2.4 hours performing 30 hops and exploring 150 meters on the surface of the Moon. This study shows promising results and our future work will involve developing a laboratory prototype for verification.

REFERENCES

[1] J. Thangavelautham, M. S. Robinson, A. Taits, et al., "Flying, hopping Pit-Bots for cave and lava tube exploration on the Moon and Mars" 2nd International Workshop on Instrumentation for Planetary Missions, NASA Goddard, 2014.

[2] H. Kalita, A. Ravindran, S. Morad, J. Thangavelautham, "Path Planning and Navigation Inside Off-World Lava Tubes and Caves," IEEE/ION PLANS Conference, 2018.

[3] H. Kalita, J. Thangavelautham, "Multirobot Cliff Climbing on Low-Gravity Environments," 11th NASA/ESA Conference on Adaptive Hardware and Systems, Pasadena, USA, 2017, 24-27 July.

[4] H. Kalita, A. S. Gholap, J. Thangavelautham, "Dynamics and Control of a Hopping Robot for Extreme Environment Exploration on the Moon and Mars," IEEE Aerospace Conference, Big Sky, USA, 2020, 7-14 March.

[5] F. Michaud, J. de Lafontaine, S. Caron, "A Spherical Robot for Planetary Surface Exploration," 6th International Symposium on Artificial Intelligence and Robotics & Automation in Space, June 2001.

[6] C. Batten, D. Wentzlaff, "Kichbot: A Spherical Autonomous Robot," MIT Technical Report, 2001.

[7] B. Chemel, E. Mutschler, H. Schempf, "Cyclops: Miniature Robotic Reconnaissance System," IEEE International Conference on Robotics & Automation, May 1999.

[8] Jeffrey Antol, "A New Vehicle for Planetary Surface Exploration: The Mars Tumbleweed," 1st Space Exploration Conference, 2005.

[9] Goran Jurisa Basic, "Power-scavenging Tumbleweed Rover," MASc Thesis, University of Toronto, 2010.

[10] Y. Xu, K. W. Au, G. C. Nandy, H. B. Brown, "Analysisof Actuation and Dynamic Balancing for a Single Wheel Robot," IEEE/RSJ International Conference on Intelligent Robots and Systems, October 1998.

[11] M. Pavone, J. C. Castillo-Rogez, I. A. D. Nesnas, J. A. Hoffman, N. J. Strange, "Spacecraft/Rover Hybrids for the Exploration of Small Solar System Bodies," IEEE Aerospace Conference, 2013.

[12] D. H. Kim et al., "Mechanism, control, and visual management of a jumping robot," Mechatronics, 2008.

[13] E. Dupius, S. Montminy, P. Allard, "Hopping robot for planetary exploration," 8th iSAIRAS, September 2005.

[14] S. Dubowsky, K. Iagnemma, et al., "A concept Mission: Microbots for Large-Scale Planetary Surface and Subsurface Exploration," Space Technology and Applications International Forum, 2005.

[15] S. B. Kesner, J. Plante, P. J. Boston, T. Fabian, S. Dubowsky, "Mobility and Power Feasibility of a Microbot Team System for Extraterrestrial Cave Exploration," IEEE Int.Conf.on Robotics and Automation, 2007.

[16] H. Kalita, J. Thangavelautham, "Automated Multidisciplinary Design and Control of Hopping Robots for Exploration of Extreme Environments on the Moon and Mars," 70th International Astronautical Congress (IAC), Washington D.C., USA, 2019, 21-25 October.

BIOGRAPHY

Himangshu Kalita *received a B.Tech. in Mechanical Engineering from National Institute of Technology, Silchar, India in 2012. He is presently pursuing his Ph.D. in Mechanical Engineering from the University of Arizona in the Space and Terrestrial Robotic Exploration (SpaceTREx) Laboratory. His research interests include dynamics and control, space robotics, machine learning and automated design.*

George Stancu *is pursuing a B.S. in Aerospace Engineering at the University of Arizona. He is an undergraduate research assistant at the University's Space and Terrestrial Robotic Exploration (SpaceTREx) Laboratory. After graduation, he hopes to start a career in exploring and developing other planets.*

Jekanthan Thangavelautham *has a background in aerospace engineering from the University of Toronto. He worked on Canadarm, Canadarm 2 and the DARPA Orbital Express missions at MDA Space Missions. Jekan obtained his Ph.D. in space robotics at the University of Toronto Institute for Aerospace Studies (UTIAS) and dis his postdoctoral training at MIT's Field and Space Robotics Laboratory (FSRL). Jekan Thanga is an assistant professor and heads the Space and Terrestrial Robotic Exploration (SpaceTREx) Laboratory at the University of Arizona. He is the Engineering Principal Investigator on the AOSAT I CubeSat Centrifuge mission and is a Co-Investigator on SWIMSat, an Airforce CubeSat mission concept to monitor space threats.*

View publication stats